

Observing the Holographic Nature of Quantum Spacetime

James L. Sebald

August 9, 2013

The measurement of holographic noise offers the potential to make a major step forward in the understanding of how the laws of general relativity and quantum mechanics may unify at the Planck scale. Fermi National Laboratory's Holometer experiment utilizes two nested Michelson interferometers to attempt to measure an interference pattern in a recombined monochromatic beam resulting from a new transverse uncertainty in quantum position predicted by the theory of holographic noise. The signals from these two interferometers will be dually analyzed under spectral analysis in an attempt to isolate a non-filterable background noise. The isolation of this fundamental noise will confirm the random walk transverse jittering effects in measurements predicted by holographic noise theory, and mark a support for validity of the existence of the holographic principle. If this noise can in fact be measured it will mark a first real understanding of how a classical spacetime structure emerges at the quantum level, as well as act for the first experimental support for the holographic principle.

An Emergent Spacetime

In the classic spacetime predicted by general relativity, position is conceptualized as the real projection of pointlike events on a continuous manifold. This deterministic definition of position strongly contradicts the quantum theory of position in which it is defined not as coordinate event, but rather the result of an interaction between bodies producing an uncertainty in spatial coordinates. This uncertainty leads to a current lack in the fundamental understanding of quantum positioning. The discrepancy between these two definitions leads to a current ambiguity in the quantum geometry of the local metric. Furthermore, how a classical 3+1 spacetime could emerge from this quantum metric is also currently not fully understood.

To search for a metric covariant in both theories, the limiting case where the idea of length in both classic spacetime (via the Schwarzschild Radius) and classic quantum mechanics (via the wavelength of a quantum particle) converge at the quantum level needs to be investigated; the realms of these two length scales meet at the Planck scale, the physics below which there is currently no understanding. The theory of the holographic noise is a result of an attempt to converge these two realms of physics, where spacetime becomes pixelated and two dimensional at the Planck scale.¹

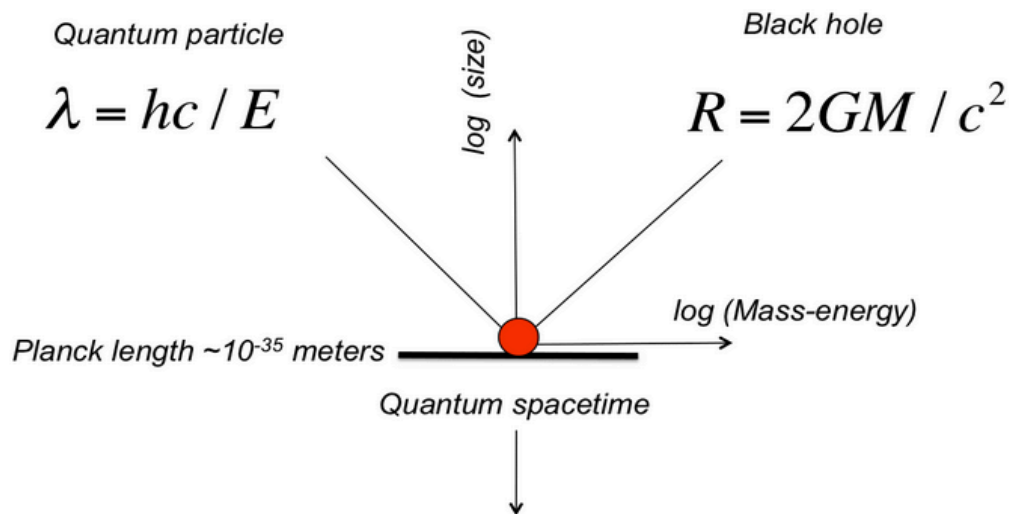


FIG. 1: Relationship between quantum mechanics and gravity through the Planck scale. The vertical axis corresponds to a definition of length, and the horizontal axis a definition of energy for respective quantum and gravitational systems. The separate systems meet at the Planck scale where the laws of quantum mechanics and gravity are expected to unify.

In this pixelization of the metric, because an object becomes localized within a Planck unit area, the momentum of said particle must delocalize. This uncertainty prevents the measurement of a body in two directions at the same time with perfect accuracy, thus giving the particle a transverse uncertainty and producing a random walk effect in measurements. This therefore leads to a new uncertainty principle for perpendicular directions, where for a given z directional propagating particle,

$$\Delta x \Delta y \geq \frac{L \cdot l_p}{2}$$

Where L is the displacement along the direction of propagation, and l_p is the Planck length. This random walk effect would theoretically manifest itself as both a fundamental and uniform background noise in positional measurements in high-precision experiments.

To understand how this uncertainty arises, one needs to consider the wave-like nature of a propagating particle. If spatial locations are encoded on wavefronts as the holographic principle suggests, then this localization in the transverse wavefront range will lead to a delocalization in transverse momentum with accordance to the classic Heisenberg uncertainty principle. The transverse localization of wavefronts therefore leads to a superposition of forward propagating waves. When a measurement is made of this superposition, the wave function must collapse into one of the transverse displacements of its constituents. Therefore with each successful wavefront a different transverse position can be measured, leading to an observable noise in measurement.

It is this uncertainty or “blurriness” in physical measurements that can be holistically linked to the holographic principle through the laws of thermodynamics. The theorized holographic principle also stemming from the unification of general relativity and quantum mechanics predicts the pixelation of the cosmological horizon encompassing the observable universe. As shown by Bekenstein and Hawking in their analysis of black hole thermodynamics, information is encoded on the surface of a given horizon to preserve the conservation of the information of the constituents from with the horizon itself. If this theory is extrapolated to the cosmological horizon, then the 3D world we perceive around us should truly be a 2D encoding stored on the horizon. If our 3D world is understood as an emergent entity from this 2D definition, then the uncertainties seen on the quantum level can become to be understood. If information defined by 2 degrees of

freedom were to emerge into a system with an extra degree of freedom (our 3D world), then said information would be underconstrained, and an uncertainty (or blurriness) would become inherent. It is through this holistic connection that the measurement in the fundamental blurriness of holographic noise could be used to support the holographic principle.

Measuring Holographic Noise

Fermilab's holometer utilizes two nested Michelson interferometers to measure the power of a monochromatic beam split and recombined by a beam splitter. The optical layout of this system can be seen in Figure 2 below. The laser source sends a beam of monochromatic light (1064 nm) into the interferometer through a power-recycling mirror to monitor the number of absorbed photons. Upon entering the interferometer the beam is divided by a half silvered mirror beam splitter that separates the beam down two separate arm lengths with equivalent probability. The separated beams then reflect off mirrors at the end of each arm length, and then recombine again at the beam splitter. The state of the combined beam is dependent on the difference in path length between the two arms. The arm lengths have been designed to have a path length difference equal to half of the beams wavelength. Classically this path length difference would lead to complete interference between the combined waves. However, if the theory of holographic noise is correct, this path length difference will be constantly fluctuating in accordance to introduced uncertainty by the theory.

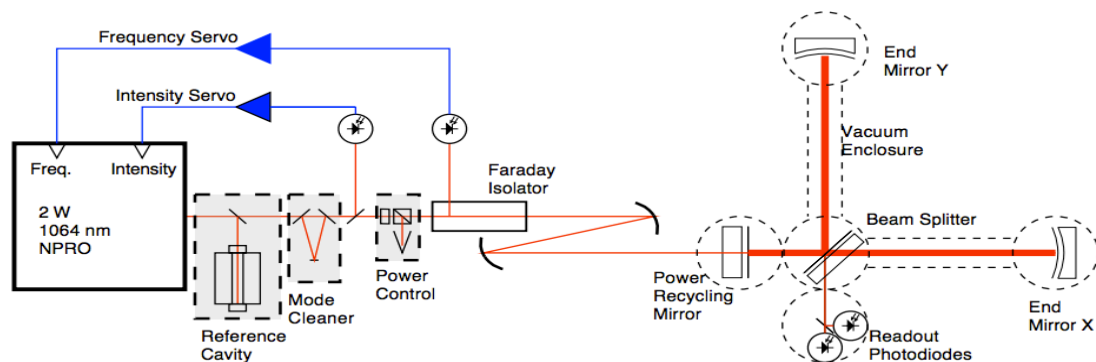


FIG. 2: The optical layout for the holometer. The laser's 2W 1064 nm light shines through three control mechanisms (reference cavity, mode cleaner, and power control), where it is focused through a Faraday Isolator and then introduced into the interferometer via a recycling mirror. The beam is then split at the beams splitter where it travels down two separate arms, reflects, and then recombines at the beams splitter and measured at the photodiodes.

These fluctuations will stem from the transverse uncertainty in both beam splitter arms. As can be seen below in Figure 3, a transverse uncertainty in one arm (δ_1 and $L1$) will produce a change the in net path length in the secondary arm ($L2$) and vice versa. These changes in net path length will prevent complete interference when the beams are recombined at the beam splitter and, as a result, a residual signal will remain signaling the existence of holographic noise.

In order to simplify the task of isolating the desired holographic noise signal, a secondary interferometer is used to exploit the causal effects of locality. If two interferometers are adequately close, the null wavefronts of each interferometer's beam will become casually correlated where individual wavefronts will collapse in correlation between the two interferometers. Due to this causality, the holographic noise form each of these two interferometers will be a correlated signal. If the overall signals from these two interferometers are analyzed under spectral analysis with a cross-coherence calculation, only the holographic noise signal and other correlated noise will remain. If this additional correlated noise can be reduced, a predictable coherent signal should remain thus offering a measurement of holographic noise.

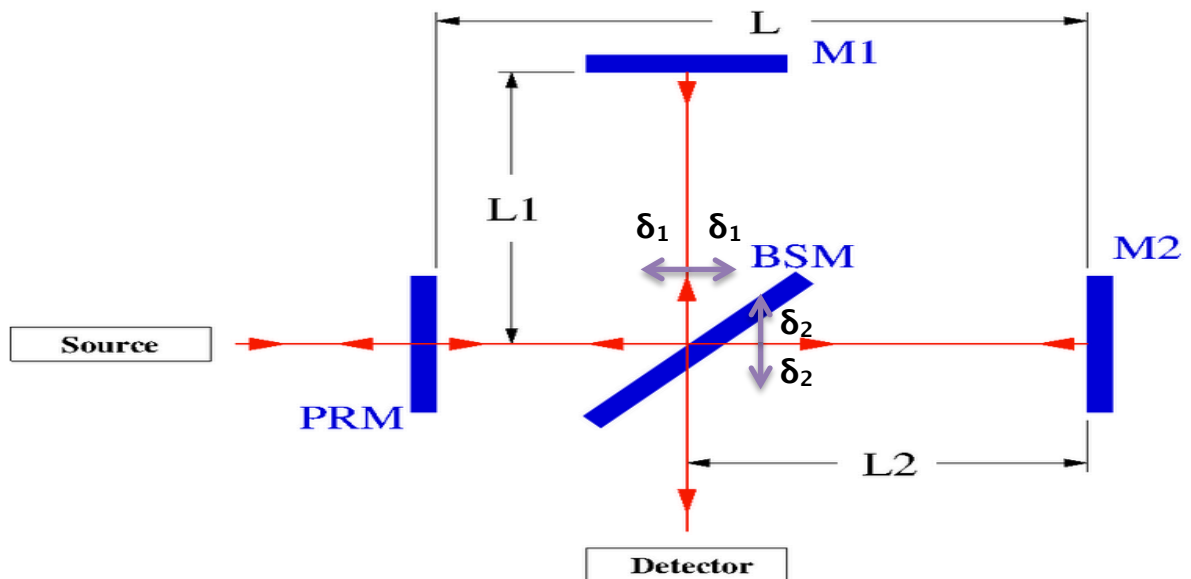


FIG. 3: Diagram how of transverse uncertainties are introduced to interferometer experiments. The transverse uncertainty in propagation of a beam in one arm length will alter the effective path length of the secondary beam and vice versa. These changing path lengths will a small variation from the expected interference of the combined beams.

Although these high-precision measurement techniques are not new to interferometer experiments, other high-precision experiments oftentimes avoid the co-located interferometer designs necessary to see holographic noise. Additionally, these previous measurements such as in the gravitational wave interferometer LIGO did not incorporate a sufficiently strong enough power-recycling device to aid in isolating the holographic noise signal. The lack of these criteria rules out other high-precision interferometer experiments used in other fields as possible confirmations holographic noise.

The Fundamental Signal

Photodiodes will be used to measure the incoming power of the beams at each of the dark ports in the interferometers, converting the measured power of the laser to a corresponding voltage. To discern individual sources within the signal, a Fourier Transformation is used to convert the signal from a time domain signal to a frequency domain signal. It is this frequency domain signal that will be analyzed for holographic noise by using spectral analysis to examine the signal's power spectra [2], cross power spectra [2], cross-coherence [3], and phase spectra. The calculations for each of these three spectra can be seen below.

$$PS = \sqrt{|\langle x_i x_j^* \rangle|} \quad [2]$$

$$CC = \frac{|\langle x_i x_j^* \rangle|}{\sqrt{\langle x_i x_i^* \rangle \langle x_j x_j^* \rangle}} \quad [3]$$

The power spectra will be measured by measuring the power of the monochromatic beam at four different channels, with each channel located at one of the two interferometer's two splitter arms. The signal from each of these channels will be used to calculate a cross power spectra by comparing the power spectra of each channel in combination with each other, leading to six comparisons in total. These signal comparison combinations will also be used to analyze the cross-coherence between channels. The holographic noise signal we are seeking will appear in both the cross-power spectra and cross-coherence spectra. Finally the phase spectra of each of these combinations will also be analyzed to insure that the end signal is in fact uncorrelated.

Although the holographic noise signal is theorized to be constant across all frequencies, the sensitivity of the interferometer will lead to a bias in the observed frequency range. These interferometers have no sensitivity at frequencies directly proportional to the frequency at which photons making a round trip from the beam splitter to the end mirror and back. This value will take the form,

$$f = \frac{n \cdot c}{2L}$$

With n being some integer, c being the speed of light, and L the length of the interferometer arm, comes out to be integer values of 3.75Mhz. The amplitude of the noise is predicted to be fixed by the Planck scale, with an expected value of about $\sqrt{lp \cdot L}$. With these predictions, the expected spectrum of the holographic noise can be seen in the Figure 4 below, where the amplitude of the noise has been multiplied by the interferometer's limited efficiency.

Because the frequency spectrum of holographic noise is difficult to measure with a single detector, the cross-correlation of the noise will be measured between the two adjacent interferometers. The component of the noise due to the holographic jitter of the common underlying spacetime grows coherently and linearly with time, in comparison to the product of the uncorrelated random noise in the two interferometers that sums with a random phase and grows as the square root of time. This leads to a separate time dependence between the two noise spectra and allows for the holographic noise signal to be isolated by averaging over long scale data acquisitions. The theorized isolated spectra for holographic noise can be seen in the Figure 4 below.

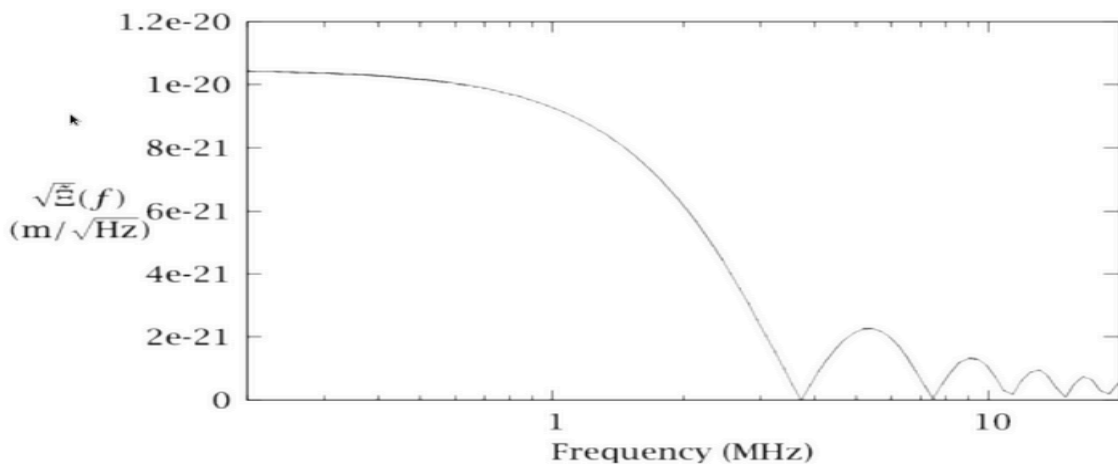


Figure 4 Predicted measured frequency spectrum of holographic noise. The component of the noise due to the holographic jitter of the common underlying spacetime will sum coherently and grow linearly with time, while the product of the uncorrelated random noise in the two devices will sum with a random phase and grow only as the square root of time. In this way, the correlated noise can be easily isolated.

Three factors will be used to confirm that a holographic noise signal has been found. These are:

1. The strength of the end signal as compared to the theoretical predictions.
2. The shape of the end spectra.
3. The modulation of the correlation between two different interferometer configurations.

Multi-Channel Analysis

The observation of how the autocorrelation functions at each of the dark ports cross-correlates with one another in a live setting is key to the success of the experiment. To analyze these things efficiently, a GUI will need to be made allowing for instantaneous analysis of each of these key values. This GUI will take the form of a 4x4 grid, where each cell along the diagonal corresponds to a live plot of an autocorrelation acquisition at on of each of the four detectors in the experiment. Each off-diagonal entry contains a live plot of the cross-correlated statistics from the two respective autocorrelation detectors. See below for a visual concerning the layout of the GUI.

It should be noted that the GUI has a few key aspects critical to understand in its usage. Primarily with all 16 plots activated, the system significantly slows down. This leads to the addition of the button control panel, which allows plots to be turned on and off individually. Additionally, each individual plot can be opened in an additional larger window to enhance the plots visibility. As these functions drop off with time, their overall amplitudes will progressively decrease, inspiring the addition of an Auto Scaling button. This button will scale each plot in such a way to maximize the size of each plot in the allowed space. By default, this GUI acts in a monitoring mode where all plots are updated live, with the scaling in each plot adjusting with the supplied data.

The GUI has additionally been built in with a user interface allowing users to adjust any free parameters of the GUI before taking data. This interface is divided into four subcategories: Data Source Selection, Time Variables, Device Settings, and Writing Options. Upon selection of these options, the data acquisition system will adjust and begin taking data accordingly. A summary of these menus can be seen on the next two pages.

Data Source Selection	
use_real_5122	Turns off any virtual simulation software, and activates all live feed digitizers
use_realtime_mode	Limits incoming data sets to allow for manageable flow rate for analysis
use_start_trig	Synchronizes time rate for each GPS
Use_gpa_sync	Synchronizes initial time for each GPS

Table I. The Data Source Selection Menu: Houses setting used to control equipment software used in the data acquisition process.

Time Variables	
Integration Time	Sets total running time for data acquisition
Accumulation Time	Sets how long each data set will be averaged over
Frame Overlap Fraction	Prevents aliasing effects from non-periodic functions discrete functions by overlapping sequential data sets by given fraction
FFT Size	Sets size of datasets used in Fast Fourier Transformation

Table II. The Time Variable Menu: Houses settings that control the way in which the acquisition system both acquires and prepares data for analysis.

Device Settings	
GPS Name	Set GPS by name
Frequency	Sampling frequency for acquisition system
DC Offset	Add a deviation to digitizer's measured voltages
Scaling	Scales the signal by given factor
Coupling	Toggle between different pass filters
Voltage Range	Set bit resolution
Impedance	Sets impedance of sources

Table III. The Device Settings Menu: Controls the individual settings for both acquisition devices (Lester and Thurgood); it should be noted that these settings need to be adjusted for both devices separately, and before each acquisition session.

Writer Settings	
use_hdf5_writer	Activates automatics file maker
Time Intervals	Sets file creation time interval
Database log file	Set name of generated log file

Table IV. The writing settings menu controls how individual data files are formatted and saved.

Final Remarks

From the cross-correlated analysis of signals from both photodiodes, a noise signal can be found. If external sources from this signal can be reduced, it is theorized a fundamental signal will reside. This fundamental signal would be caused by a new uncertainty in transverse measurements explainable by the holographic noise theory. If this fundamental noise fulfills the three factors of criteria, the holographic noise theory proves valid, and one of the first experimental supports for the holographic principle will be found. This discovery will be a significant clue to the quantum origins of spacetime, as well as to speak to the structure of spacetime at gravitational horizons, as it will reveal the first real concrete signature of the holographic nature of spacetime at the quantum level. From this deeper understanding of spacetime at the most fundamental of levels, the two great theories of general relativity and quantum mechanics will finally take one great step towards unification and offer an insight into a single unified theory.

ACKNOWLEDGEMENTS

This work was supported in part by the U.S. Department of Energy, Office of Science, Office of Workforce Development for Teachers and Scientists (WDTS) under the Science Undergraduate Laboratory Internship (SULI) Program.

I would like to give thanks to Chris Stoughton and Jonathon Richardson whose excellent mentoring made this project possible, Eric Ramberg for giving me the opportunity to work at this amazing institute, and Carol Angarola whose program coordination made all the work fluid. Each of these individuals made this research experience, undeniably, an excellent one.

REFERENCES

- [1] Craig Hogan, "Spacetime Indeterminacy and Holographic Noise," 13 June 2007, arXiv:0706.1999.
- [2] Craig Hogan et al., "The Fermilab Holometer," 2009, Fermilab-Proposal-0990.
- [3] Craig Hogan, "Interferometers as Probes of Planckian Quantum Geometry," 2012, DOI: 10.1103/PhysRevD.85.064007.